Journal of Sound and Vibration (2000) **230**(5), 1119–1145
doi:10.1006/jsvi.1999.2670, available online at http://www.idealibrary.com on IDEAL®

FINITE DIFFERENCE ANALYSIS OF ROTATIONALLY SYMMETRIC SHELLS USING VARIABLE NODE POINT SPACINGS

T. A. SMITH

U.S. Army Aviation and Missile Command, Redstone Arsenal, AL 35898, *U.S.A.*

(*Received* 11 *November* 1996, *and in final form* 13 *September* 1999)

The system of equations for the analysis of rotationally symmetric shells under time-dependent or static surface loadings has been formulated with the transverse, meridional, and circumferential displacements as the dependent variables. All loading functions must be continuous. The thickness h of the shell may vary along the meridian. Four of the eight natural boundary conditions will be prescribed as time-dependent boundary conditions at each boundary edge of the shell. Surface loadings and inertia forces in the three displacement directions of the shell have been considered. Fourier series are used in the circumferential direction of the shell. Solutions for each Fourier component are found by replacing all derivatives by their finite difference equivalents and solving the resulting system of algebraic equations at successive increments of the time variable. The complete system of equations is solved implicitly for the first time increment, while explicit relations are used to determine the three primary displacements within the boundary edges of the shell for the second and succeeding time increments. The remaining unspecified primary variables are then determined by separate implicit solutions at each boundary for the second and succeeding time increments. Subsequently, all remaining primary and secondary variables are found explicitly. A variable node point spacing may be specified over the full range of the spatial finite difference mesh. A numerical stability criterion which will ensure stable solutions for selected time increments and spatial meshes has been derived and found to agree with results for typical example solutions. Numerical solutions obtained with the computer program which accompanies this development have been found to be stable and in agreement for a wide range of practical values of both spatial and time increments for typical shells and loadings. Static and dynamic solutions for a parabolic shell with fixed boundary conditions at one edge and free boundary conditions at the other edge have been obtained using both constant and variable node point spacings and presented as examples.

1. INTRODUCTION

In the absence of closed-form solutions for the general shell problem, several investigators have obtained solutions by numerical methods. These investigators include Penny [1], who solved the symmetric bending problem of a general shell in 1961 by finite differences; Radkowski *et al.* [2], who solved the axisymmetric static

0022-460X/00/101119 + 27 $35.00/0

problem in 1962 by finite differences; and Budiansky and Radkowski [3], who employed finite difference methods to solve the unsymmetrical static bending problem in 1963.

The solution to the static problem of rotationally symmetric shells of revolution subjected to both symmetrical and non-symmetrical loading was obtained also by Kalnins [4] in 1964. Starting with the equations of the linear classical bending theory of shells, in which the thermal effects were included, Kalnins derived a system of eight first order ordinary differential equations which he solved by direct numerical integration over preselected segments of the shell. Gaussian elimination was used to solve the resulting system of matrix equations obtained by providing continuity of the fundamental variables at the segmental division points.

In 1965, Percy *et al.* [5] also developed a finite element technique for the analysis of shells of revolution under both axisymmetric and asymmetric static loading by idealizing the shell as a series of conical frusta.

The solution for the free vibration characteristics of rotationally symmetric shells with meridional variations in the shell parameters by means of his multisegment direct numerical integration approach was also obtained by Kalnins [6] in 1964. Subsequently, in 1965, the solution for the response of an arbitrary shell subjected to time-dependent surface loadings was obtained by Kraus and Kalnins [7] by means of the classical method of spectral representation. The solution was expanded in terms of the modes of free vibration as determined previously by Kalnins [6], and the orthogonality of the normal modes was proved for an arbitrary shell.

In 1966, Klein [8] also published an article in which he describes a matrix displacement finite element approach to the linear elastic analysis of multilayer shells of revolution under axisymmetric and asymmetric dynamic and impulsive loadings. The method of solution involves the idealization of the shell as a series of conical frusta joined at nodal circles.

Subsequently, Smith [9, 10] published reports containing numerical procedures for the analysis of rotationally symmetric thin shells of revolution under time-dependent impulsive and thermal loadings. The field equations consisted of eight first order partial differential equations with respect to the meridional co-ordinate of the shell, and the solution for each Fourier harmonic was obtained by employing low order finite difference representations for all time and spatial derivatives.

In 1973, Smith [11] published a report giving numerical procedures for finding the dynamic response of rotationally symmetric thin shells of revolution under time-dependent surface and thermal loadings utilizing a higher order finite difference representation of spatial derivatives than that used in references [9, 10]. The field equations consisted of eight first order differential equations, while the time derivatives were represented by ordinary backward finite differences, thus resulting in stable implicit solutions for all choices of the time increment.

In 1975, Radwan and Genin [12] published their development of the equations for the determination of the non-linear response of thin elastic shells of arbitrary geometry under either static or dynamic loading through the use of assumed,

known, or calculated mode shape functions. The geometric non-linearities were considered by employing the strain-displacement relations of the Sanders–Koiter non-linear shell theory. Introduction of the mode shape functions into the system of governing equations leads to a system of ordinary differential equations for the generalized time co-ordinates.

In 1977, Smith [13, 14] published reports giving numerical procedures for the analysis of rotationally symmetric thin shells of revolution under continuous time dependent distributed surface and thermal loadings by use of both a high order finite difference representation of the spatial derivatives and explicit relations for the dependent variables for the second and succeeding time increments.

In 1983, Chang *et al.* [15] published their development of procedures for the linear dynamic analysis of rotationally symmetric shells using finite elements and modal expansion. Doubly-curved axisymmetric shell finite elements with the loadings and displacements expanded in Fourier series in the circumferential direction of the shell and with the requisite number of frequencies and mode shapes for the meridional displacements for each Fourier number were used in the formulation of the system of equations.

In 1983, Smith [16, 17] presented numerical formulations for determining both static and dynamic solutions for rotationally symmetric thin shells of revolution subjected to distributed loadings which may be discontinuous. Correct and converging solutions are obtained by formulating the governing equations in terms of the transverse, meridional, and circumferential displacements as the dependent variables and by using ordinary finite difference representations based upon a constant nodal point spacing for the derivatives.

In 1986, Manteuffel and White [18] published the results of their studies relative to finite difference solution of single second-order differential equations using non-uniform meshes. Those studies concern the truncation errors and order of accuracy of solutions obtained by some commonly used finite difference representations. It is concluded therein that most finite difference schemes yield second-order-accurate solutions despite the authors' finding therein that the associated truncation error is only of the first order.

In 1990, Smith [19] completed development of procedures for determining the total shell response of any rotationally symmetric general shell under time-dependent (or static) surface loadings by the modal superposition method. The solutions treated there are accomplished by first determining the free vibration characteristics of the shell through the use of influence coefficients for the discretized shell. Subsequently, the time-dependent solution is expanded in terms of the modes of free vibration of the shell to obtain the total shell response as a summation of the several modal contributions. The procedures used are analogous to procedures given by Norris *et al.* [20] and illustrated therein by a simply supported beam structure.

In 1992, Manteuffel and White [21] generalized their studies of reference [18] by considering the two-point boundary value problem for a single differential equation of arbitrary order when solved by use of irregular finite difference meshes. These studies are implemented by first writing the high-order equation as a system of first order differential equations and then proceeding with an analysis of the

first-order equations by finite difference schemes. In particular, it is found therein that if the first-order system is represented by a centered Euler scheme, solutions will be second-order-accurate despite possibly inconsistent truncation errors.

In 1994, Smith [22] published a second report in which numerical procedures were demonstrated for determining the dynamic response of rotationally symmetric open-ended thin shells of revolution under continuous time-dependent distributed surface and thermal loadings by use of a high order finite difference representation of the spatial derivatives and explicit expressions for the displacement variables within the boundary edges of the shell for the second and succeeding time increments. Reference [22] constitutes a revision to the formulation and accompanying program of reference [13] to provide stable solutions for either free, partially restrained, or fully restrained boundaries.

In 1995, Smith [23] published his development of the formulation for the finite difference analysis of general open-ended rotationally symmetric shells under either static or time dependent continuous loadings for which a variable nodal point spacing may be used in the meridional finite difference mesh. As in reference [16], the governing differential equations were formulated in terms of the displacements w, u_ϕ, and u_θ and Fourier expansion was used in the circumferential direction of the shell. The complete system of equations is solved implicitly for the first time increment after using low order central difference variable nodal point spacing representations for all spatial derivatives and using ordinary time derivatives. Explicit relations are used to obtain the displacements w_n, $u_{\phi n}$, and $u_{\theta n}$ within the boundary edges of the shell for the second and later time increments. The remaining fundamental variables are, for the second and later time increments, found from separate implicit solutions at each boundary. The selection of a time increment which, in conjunction with the spatial finite difference mesh, is expected to produce numerically stable solutions is obtained from an explicit empirical relation for the time increment in terms of the minimum spatial increment.

In 1997, Smith [24] published his development of improvements to the formulation and finite difference representations used in reference [9]. These improvements included the addition of inertia forces and applied loadings in the circumferential direction of the shell and incorporation of the meridional coordinate s as the spatial variable in lieu of the co-ordinate z along the axis of symmetry of the shell. Solution formulations by both the explicit method and the implicit method for time-dependent loadings are included. Solutions found by the two methods show favorable comparison.

In 1998, Smith [25] published a second report on the finite difference analysis of rotationally symmetric shells under either static or dynamic loadings for which a variable node point spacing may be used in the spatial finite difference mesh and for which an eigenvalue analysis of the explicit coefficient matrices to evaluate numerical stability (or instability) of the solution for given choices of spatial mesh and time increment for the case of dynamic loadings was incorporated. Additionally, the finite difference representation for second and fourth derivatives was altered from that used in reference [23] to provide a consistent order of truncation error for all derivatives, thus departing from a central derivative representation for second and fourth derivatives.

Among references [1–25] above which provide solutions of the shell equations by the finite difference method, only references [23, 25] use a variable node point spacing in the finite difference mesh. Finite difference solutions of the shell equations by the formulations used in the others of these references are based upon use of a constant node point spacing. The studies embodied in references [18, 21] together with similar uncited references in the open literature relate to finite difference analysis of particular single equations using non-uniform meshes, none of which pertain to either static or dynamic finite difference analysis of the shell equations using a variable node point spacing. The differential equations themselves are the same for references [16, 23, 25]; but, as indicated previously, a variable node point spacing finite difference mesh is incorporated only in the formulations of references [23, 25]. It is of interest to note that typical solutions as reported in this article are identical for cases of constant node point spacings when found by the programs of references [23, 25] and that the results agree to 3 and 4 significant figures when a variable node point spacing is used. The author is also not aware of the publication in the open literature of any findings pertaining directly to numerical stability analysis of the finite difference equations for shell structures under dynamic loadings. The purpose of this article is therefore to present the development of procedures for the finite difference analysis of rotationally symmetric shells for which node point spacings may be arbitrary throughout the mesh and for which a criterion for numerical stability or instability of the solution is given as presented by the author in reference [25].

2. GOVERNING DIFFERENTIAL EQUATIONS

Our system of governing equations will be based on the linear classical theory of shells as given by Reissner [26]. Surface loadings and inertia forces in each of the three displacement directions w, u_ϕ, and u_θ will be considered. All rotary inertia terms will be neglected.

The thickness h of the shell may vary along the meridian, and we assume continuity of h and its derivatives through the second order. We assume that $\varrho/R_\phi \ll 1$ and that $\varrho/R_\theta \ll 1$, where ϱ is measured from the shell middle surface on a normal to the middle surface and is positive outward. Hence, we take $N_{\theta\phi} = N_{\phi\theta}$ and $M_{\theta\phi} = M_{\phi\theta}$.

The geometry and co-ordinate system for the middle surface of our shell is shown in Figure 1. Shell element membrane and shear forces are shown in Figure 2, and shell element bending and twisting moments are shown in Figure 3.

The position of any point on the middle surface of the shell may be defined by the co-ordinates θ and z. The undeformed geometry of the shell's middle surface will accordingly be defined by the function $r = r(z)$. However, either the co-ordinate ϕ or the co-ordinate s may be used in lieu of the co-ordinate z. We choose to develop our governing equations with the meridional co-ordinate s as the independent variable. This complete development is given in reference [25].

We assume that the material of the shell is both homogeneous and isotropic. We neglect the effects of the thermal loadings on E, ν, and α and assume that E, ν, and α are constant.

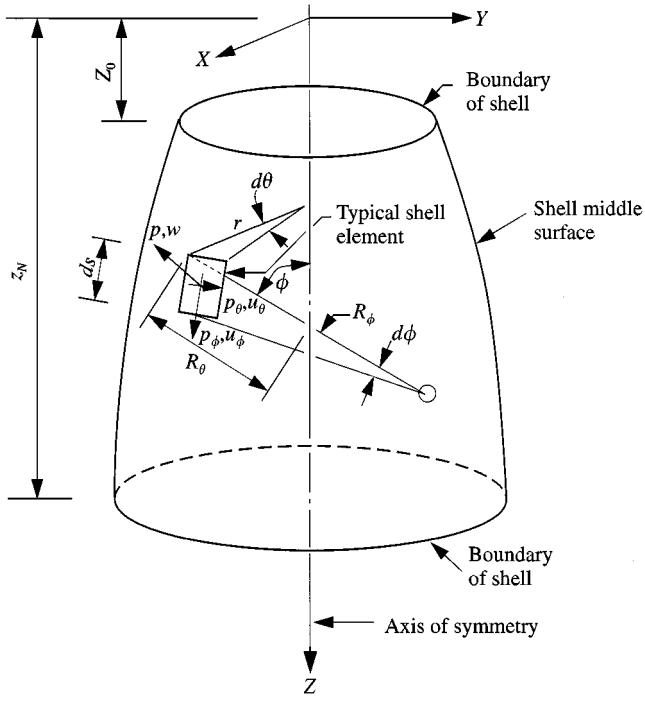

Figure 1. Typical shell of revolution.

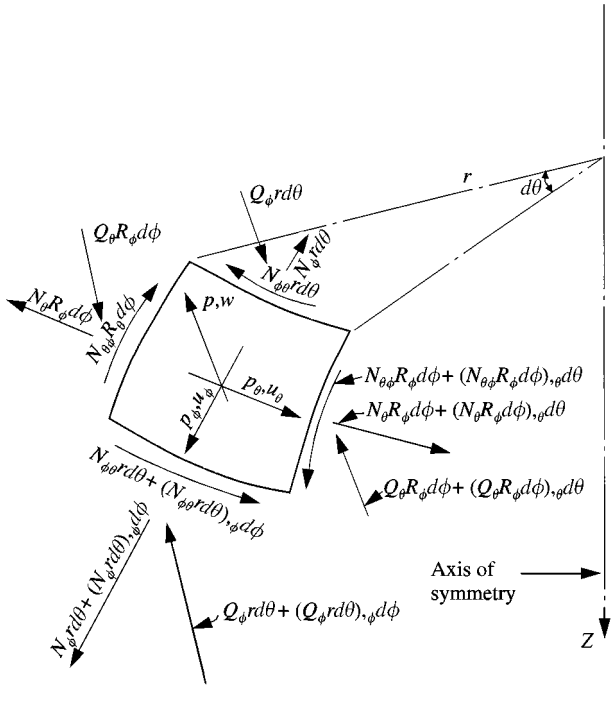

Figure 2. Shell element membrane and shear forces.

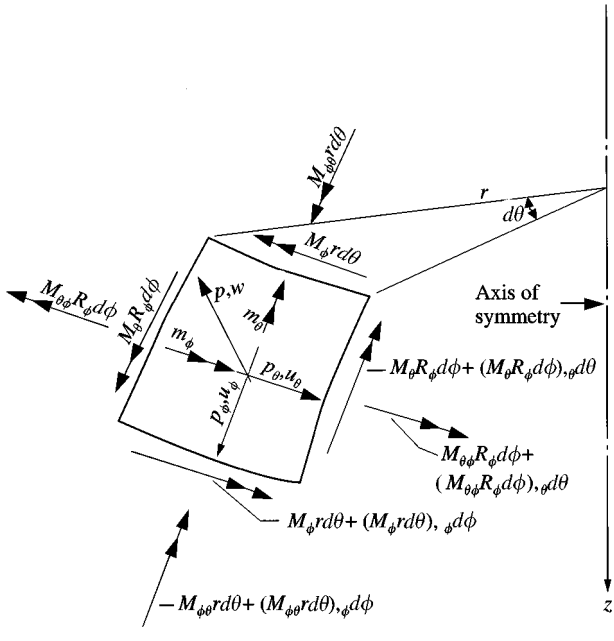

Figure 3. Shell element bending and twisting moments.

Our system of governing equations involving the stress–strain relations, strain-displacement relations, and the force equilibrium equations can be reduced to a system of equations consisting of three differential equations in terms of three unknown displacements w, u_ϕ, and u_θ. It will be convenient, however, to incorporate into our system of equations as unknowns at the boundary edges of the shell the remaining quantities which enter into the natural boundary conditions at $\phi =$ constant. In the classical theory of shells, the quantities which appear in the natural boundary conditions on a rotationally symmetric edge of a shell of revolution are the generalized displacements w, u_ϕ, u_θ, and β_ϕ and the generalized forces Q, N_ϕ, N, and M_ϕ. Thus, our system of equations will consist of the three field equations in terms of the displacements w, u_ϕ and u_θ and a definition of β_ϕ, Q, N_ϕ, N, and M_ϕ at each boundary in terms of the displacements w, u_ϕ, and u_θ together with four equations prescribing the four of the appropriate quantities w, u_ϕ, u_θ, β_ϕ, Q, N_ϕ, N, and M_ϕ at each boundary of the shell. The quantities N and Q are the effective shear resultants and are defined as

$$N = N_{\theta\phi} + \frac{\sin\phi}{r} M_{\theta\phi}, \quad Q = Q_\phi + \frac{1}{r} M_{\theta\phi,\theta}. \tag{1,2}$$

We define the quantities w, u_ϕ, u_θ, β_ϕ, Q, N_ϕ, N, and M_ϕ to constitute the primary variables in our system of equations. The variables β_θ, N_θ, $N_{\theta\phi}$, M_θ, $M_{\theta\phi}$, Q_ϕ, and Q_θ are designated as the secondary variables. From two of our five useful equations

of equilibrium, we find

$$Q_\phi = \frac{1}{r} M_{\theta\phi,\theta} + M_{\phi,s} + \frac{\cos\phi}{r}(M_\phi - M_\theta) + m_\phi, \tag{3}$$

$$Q_\theta = \frac{1}{r} M_{\theta,\theta} + M_{\theta\phi,s} + \frac{2\cos\phi}{r} M_{\theta\phi} + m_\theta. \tag{4}$$

By substituting equations (3) and (4) into the remaining three equations of equilibrium, we obtain three reduced equations of equilibrium in terms of the force variables. These three equations may be found in references [14, 17, 25].

To formulate our system of equations in terms of the displacements w, u_ϕ, and u_θ, we express the stress resultants N_θ, N_ϕ, $N_{\theta\phi}$, M_θ, M_ϕ, $M_{\theta\phi}$, N, and Q in terms of the displacements and substitute the appropriate quantities into the equations involving the force variables. This complete development may be found in reference [25].

Typical boundary conditions to be applied at the boundary s_0 are

$$w(s_0, \theta, t) = w'(s_0, \theta, t) \quad \text{or} \quad Q(s_0, \theta, t) = Q'(s_0, \theta, t), \tag{5a}$$

$$u_\phi(s_0, \theta, t) = u'_\phi(s_0, \theta, t) \quad \text{or} \quad N_\phi(s_0, \theta, t) = N'_\phi(s_0, \theta, t), \tag{5b}$$

$$u_\theta(s_0, \theta, t) = u'_\theta(s_0, \theta, t) \quad \text{or} \quad N(s_0, \theta, t) = N'(s_0, \theta, t), \tag{5c}$$

$$\beta_\phi(s_0, \theta, t) = \beta'_\phi(s_0, \theta, t) \quad \text{or} \quad M_\phi(s_0, \theta, t) = M'_\phi(s_0, \theta, t), \tag{5d}$$

where the primed variables indicate specified quantities and where similar conditions will be imposed at the boundary s_N.

For the initial conditions, we will prescribe initial values of the displacements and velocities in each of the co-ordinate directions w, u_ϕ, and u_θ. Thus, the initial conditions to be considered are typically

$$w(s, \theta, t_0) = w'(s, \theta, t_0), \quad \dot{w}(s, \theta, t_0) = \dot{w}'(s, \theta, t_0), \tag{6a, b}$$

where the primed variables indicate specified values of the initial displacements and velocities.

To solve our system of equations, we expand all loadings and dependent variables in the circumferential direction of the shell in Fourier series. We will truncate these infinite series at a finite number of terms for the solution of specific shell problems. We require that all loading functions be continuous.

The Fourier series representations of the loadings p_ϕ, m_ϕ, p, T_0, and T_1, the primary variables w, u_ϕ, β_ϕ, Q, N_ϕ, and M_ϕ, and the secondary variables N_θ, M_θ, and Q_ϕ are typically

$$p_\phi = \sum_{n=0}^{P} p_{\phi n}(s, t)\cos n\theta + \sum_{n=1}^{P} \bar{p}_{\phi n}(s, t)\sin n\theta. \tag{7a}$$

The loadings p_Θ and m_Θ, the primary variables u_θ and N, and the secondary variables β_θ, $N_{\Theta\phi}$, $M_{\Theta\phi}$, and Q_θ are typically

$$p_\theta = \sum_{n=1}^{P} p_{\theta n}(s,t)\sin n\theta + \sum_{n=0}^{P} \bar{p}_{\theta n}(s,t)\cos n\theta. \tag{7b}$$

Upon substituting equations (7) into our single system of equations involving θ, s, and t as the independent variables, we obtain $P+1$ separate decoupled systems of equations in the variables s and t to solve in lieu of the single system of equations in the variables θ, s, and t. For each system we obtain two separate sets of equations, one for the variables which are designated without a bar and another for the variables which are designated with a bar. Here and elsewhere in the sequel where double signs occur in the equations, the upper sign is to accompany the first set of equations and the lower sign is to apply to the second set. Single signs will apply to both sets. The rather lengthy coefficients A_1–A_{10}, B_1–B_{13}, C_1–C_9, and D_1–D_{50}, which involve geometric and material parameters, loading terms, and the Fourier component designator n, appearing in the system of equations so found for each Fourier component may be found in reference [25].

With the referenced definition of coefficients, our field equations for each Fourier component of loading are given by

$$\begin{aligned}
&- A_1 w_{n,sss} - A_2 w_{n,ss} + A_3 w_{n,s} + A_4 w_n \\
&+ A_5 u_{\phi n,ss} + A_6 u_{\phi n,s} + A_7 u_{\phi n} \pm A_8 u_{\theta n,s} \pm A_9 u_{\theta n} \\
&- \frac{\gamma h r}{g} u_{\phi n,tt} = A_{10} - r\left(p_{\phi n} + \frac{1}{R_\phi} m_{\phi n}\right),
\end{aligned} \tag{8a}$$

$$\begin{aligned}
&- B_1 w_{n,ssss} - B_2 w_{n,sss} + B_3 w_{n,ss} + B_4 w_{n,s} + B_5 w_n \\
&+ B_6 u_{\phi n,sss} + B_7 u_{\phi n,ss} + B_8 u_{\phi n,s} + B_9 u_{\phi n} \\
&\pm B_{10} u_{\theta n,ss} \pm B_{11} u_{\theta n,s} \pm B_{12} u_{\theta n} - \frac{\gamma h r}{g} w_{n,tt} = B_{13} \mp n m_{\theta n} \\
&- r(p_n + m_{\phi n,s}) - m_{\phi n}\cos\phi,
\end{aligned} \tag{8b}$$

$$\begin{aligned}
&\pm C_1 w_{n,ss} \pm C_2 w_{n,s} \mp C_3 w_n \\
&\mp C_4 u_{\phi n,s} \mp C_5 u_{\phi n} \\
&+ C_6 u_{\theta n,ss} + C_7 u_{\theta n,s} + C_8 u_{\theta n} \\
&- \frac{\gamma h r}{g} u_{\theta n,tt} = \mp C_9 - m_{\theta n}\sin\phi - r p_{\theta n}.
\end{aligned} \tag{8c}$$

The primary variables $\beta_{\phi n}$, $N_{\phi n}$, $M_{\phi n}$, N_n, and Q_n in terms of the displacements are

$$\beta_{\phi n} = - w_{n,s} + \frac{1}{R_\phi} u_{\phi n}, \tag{9a}$$

$$N_{\phi n} = K(D_1 w_n + u_{\phi n,s} + D_2 u_{\phi n} \pm D_3 u_{\theta n} - D_4 T_{0n}), \tag{9b}$$

$$M_{\phi n} = D\left(- w_{n,ss} - D_2 w_{n,s} + D_5 w_n + \frac{1}{R_\phi} u_{\phi n,s} \right.$$

$$\left. + D_6 u_{\phi^n} \pm D_7 u_{\theta n} - D_4 T_{1n} \right), \tag{9c}$$

$$N_n = \pm D_{37} w_{n,s} \mp D_{38} w_n \mp D_{39} u_{\phi n} + D_{40} u_{\theta n,s} + D_{41} u_{\theta n}, \tag{9d}$$

$$Q_n = - D w_{n,sss} - D_{42} w_{n,ss} + D_{43} w_{n,s} - D_{44} w_n$$

$$+ D_{45} u_{\phi n,ss} + D_{46} u_{\phi n,s} + D_{47} u_{\phi n}$$

$$\pm D_{48} u_{\theta n,s} \pm D_{49} u_{\theta n} - D_{50} + m_{\phi n}. \tag{9e}$$

The variables N_n and Q_n may also be given by

$$N_n = N_{\theta\phi n} + D_{36} M_{\theta\phi n}, \quad Q_n = Q_{\phi n} \pm D_{10} M_{\theta\phi n}. \tag{10a, b}$$

The secondary variables are defined in terms of the displacements in reference [25].

Equations (9) will be written for each boundary and incorporated into our system of equations for determining or defining w_n, $u_{\phi n}$, and $u_{\theta n}$ on the range of the variable s and $\beta_{\phi n}$, $N_{\phi n}$, $M_{\phi n}$, N_n, and Q_n at the boundaries of the shell. The remaining primary variables may then be found from equations (9) or (9) and (10).

Typical boundary conditions to be considered at the boundary s_0 for each Fourier harmonic are

$$w_n(s_0, t) = w'_n(s_0, t) \quad \text{or} \quad Q_n(s_0, t) = Q'_n(s_0, t), \tag{11a}$$

$$u_{\phi n}(s_0, t) = u'_{\phi n}(s_0, t) \quad \text{or} \quad N_{\phi n}(s_0, t) = N'_{\phi n}(s_0, t), \tag{11b}$$

$$u_{\theta n}(s_0, t) = u'_{\theta n}(s_0, t) \quad \text{or} \quad N_n(s_0, t) = N'_n(s_0, t), \tag{11c}$$

$$\beta_{\phi n}(s_0, t) = \beta'_{\phi n}(s_0, t) \quad \text{or} \quad M_{\phi n}(s_0, t) = M'_{\phi n}(s_0, t), \tag{11d}$$

where the primed variables denote specified quantities and where similar boundary conditions will be imposed at the boundary s_N.

The initial conditions for each Fourier harmonic are typically

$$w_n(s, t_0) = w'_n(s, t_0), \quad \dot{w}_n(s, t_0) = \dot{w}'_n(s, t_0), \tag{12a, b}$$

where the primed variables are specified quantities.

The system of equations (8–12) has been solved numerically by Smith [9, 10, 16, 17, 23] by use of ordinary constant spacing spatial finite difference representations, by Smith [11, 13, 14, 22] by use of higher order constant spacing spatial finite difference representations, and by Smith [19] by using a constant spacing ordinary spatial finite difference mesh in conjunction with the modal superposition method. Our purpose here is to present solutions by Smith [25] which permit a variable nodal point spacing over the full range of the spatial finite difference mesh, thus allowing variable and smaller spacings at and near the shell boundaries in conjunction with wider spacings at sections removed from the boundaries.

3. FINITE DIFFERENCE REPRESENTATION OF TIME AND MERIDIONAL CO-ORDINATE DERIVATIVES

Our system of equations to be solved by finite differences for each Fourier component consists of equations (8) as the field equations, equations (9) evaluated at each boundary together with four additional equations (11) prescribing four of the quantities $w_n, u_{\phi n}, u_{\theta n}, \beta_{\phi n}, N_{\phi n}, M_{\phi n}, N_n$, and Q_n at each boundary, and equations (12) defining the initial conditions. We may then determine the variables $\beta_{\phi n}, N_{\phi n}, M_{\phi n}, N_n$, and Q_n on the interval $s_0 \leqslant s \leqslant s_N$ from equations (9) or (9) and (10).

To solve these equations, we replace all derivatives in the equations by their finite difference equivalents to obtain a system of finite difference equations which may be applied at successive increments of the time variable. To write these algebraic equations, we divide the shell meridian into N variable length increments between the boundaries s_0 and s_N and extend the shell an additional distance of two increments beyond each of the boundaries s_0 and s_N of the shell as shown in Figure 4. By writing the equilibrium equations (8a) and (8c) at the $N + 3$ meridional stations on and between the points s_{-1} and s_{N+1}, equilibrium equation (8b) on and between the boundaries s_0 and s_N, equations (9) at each of the boundaries s_0 and s_N, and four of equations (11) at each boundary, we obtain $3N + 25$ equations for determining the $3N + 25$ variables at each time increment.

We represent the accelerations at the first time increment t_1 typically as

$$\ddot{w}_n(s, t_1) = \frac{2[w_n(s, t_1) - w_n(s, t_0) - (\Delta t)\dot{w}_n(s, t_0)]}{(\Delta t)^2}. \tag{13}$$

For times $t \geqslant t_0 + 2\Delta t$, we represent the accelerations in equations (8) applied on the interval $s_1 \leqslant s \leqslant s_{N-1}$ by finite central differences about the time $t - \Delta t$. Thus, typically,

$$\ddot{w}_n(s, t - \Delta t) = \frac{w_n(s, t - 2\Delta t) - 2w_n(s, t - \Delta t) + w_n(s, t)}{(\Delta t)^2}$$

$$(s_1 \leqslant s \leqslant s_{N-1};\ t \geqslant t_0 + 2\Delta t). \tag{14}$$

Upon introducing equations (14) into equations (8), we obtain explicit expressions for $w_n(s, t)$, $u_{\phi n}(s, t)$, and $u_{\theta n}(s, t)$ on the interval $s_1 \leqslant s \leqslant s_{N-1}$ for the second and succeeding time increments.

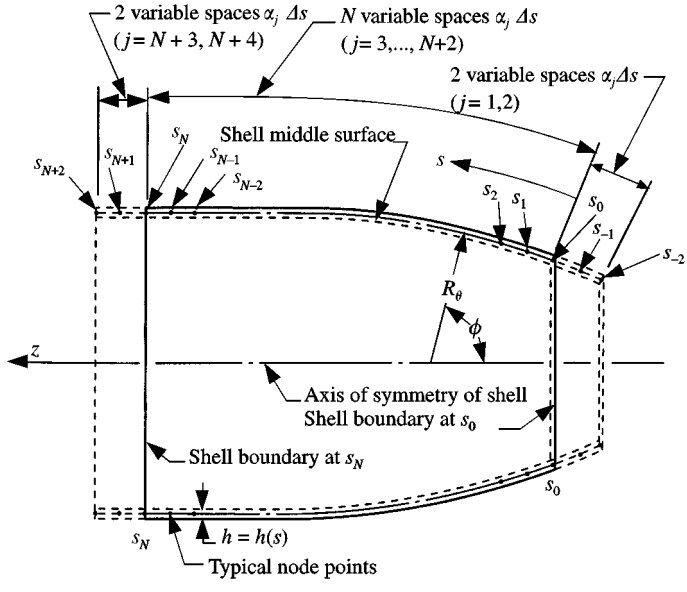

Figure 4. Node point layout for discretized shell, $\Delta s = (s_N - s_0)/N$.

Subsequent to determining our displacements on the interval $s_1 \leqslant s \leqslant s_{N-1}$, we solve implicitly, at each boundary separately, the remainder of our system of $3N + 25$ equations to determine our remaining variables on the boundaries and at all exterior points for the time t. Our accelerations appearing in equation (8) evaluated at s_0 and s_N for these systems of implicit equations will be represented typically by

$$\ddot{w}_n(s, t) = \frac{w_n(s, t - 2\Delta t) - 2w_n(s, t - \Delta t) + w_n(s, t)}{(\Delta t)^2} \quad (s = s_0; s = s_N; t \geqslant t_0 + 2\Delta t). \tag{15}$$

For our spatial finite difference mesh, we use a variable spacing finite difference representation for all derivatives. We develop these finite difference expressions by use of Taylor series expansions and solution for the undetermined coefficients in our expressions for the derivatives. This development, which provides a consistent order of truncation error for all derivatives, is given in detail in reference [25]. Our simplified expressions for all derivatives in terms of the coefficients $G_i(s)$, which are functions of the α_j and the node points s_j as shown in Figure 4 for which we evaluate the derivatives and which are defined in reference [25], are typically

$$w_{,s}(s_j) = G_1 w(s_{j-1}) + G_2 w(s_j) + G_3 w(s_{j+1}), \quad (s_{-1} \leqslant s \leqslant s_{N+1};\ -1 \leqslant j \leqslant N+1), \tag{16}$$

$$w_{,ss}(s_j) = G_4 w(s_{j-1}) + G_5 w(s_j) + G_6 w(s_{j+1}) + G_7 w(s_{j+2}),$$

$$(s_{-1} \leqslant s \leqslant s_N;\ -1 \leqslant j \leqslant N), \tag{17}$$

$$w_{,ss}(s_{N+1}) = G_8 w(s_{N-1}) + G_9 w(s_N) + G_{10} w(s_{N+1}) + G_{11} w(s_{N+2}), \tag{18}$$

$$w_{,sss}(s_j) = G_{12} w(s_{j-2}) + G_{13} w(s_{j-1}) + G_{14} w(s_j) + G_{15} w(s_{j+1}) + G_{16} w(s_{j+2}), \quad (s_0 \leqslant s \leqslant s_N; 0 \leqslant j \leqslant N), \tag{19}$$

$$w_{,sss}(s_{-1}) = G_{17} w(s_{-2}) + G_{18} w(s_{-1}) + G_{19} w(s_0) + G_{20} w(s_1) + G_{21} w(s_2), \tag{20}$$

$$w_{,sss}(s_{N+1}) = G_{22} w(s_{N-2}) + G_{23} w(s_{N-1}) + G_{24} w(s_N) + G_{25} w(s_{N+1}) + G_{26} w(s_{N+2}), \tag{21}$$

$$w_{,ssss}(s_j) = G_{27} w(s_{j-2}) + G_{28} w(s_{j-1}) + G_{29} w(s_j) + G_{30} w(s_{j+1}) + G_{31} w(s_{j+2}) + G_{32} w(s_{j+3}), (s_0 \leqslant s \leqslant s_{N-1}; 0 \leqslant j \leqslant N-1), \tag{22}$$

$$w_{,ssss}(s_N) = G_{33} w(s_{N-3}) + G_{34} w(s_{N-2}) + G_{35} w(s_{N-1}) + G_{36} w(s_N) + G_{37} w(s_{N+1}) + G_{38} w(s_{N+2}). \tag{23}$$

4. GOVERNING FINITE DIFFERENCE EQUATIONS

To convert equations (8), (9), (11), and (12) to spatial finite difference form, we make appropriate substitutions for the spatial derivatives appearing therein from equations (16–23) inclusive. The time derivatives appearing in our equations will be converted to temporal finite difference form for the first time increment by utilizing the backward temporal finite difference representations given typically by equation (13), thus rendering an implicit solution to our system of equations for the first time increment.

Further, to produce more nearly equal coefficients in our system of finite difference equations, we define new force variables to be

$$N^0_{\phi n} = N_{\phi n} \times 10^{-6},\ M^0_{\phi n} = M_{\phi n} \times 10^{-6},\ N^0_n = N_n \times 10^{-6},\ Q^0_n = Q_n \times 10^{-6}. \tag{24}$$

We also define new coefficients C^0 of the force variables to be

$$C^0(N^0_{\phi n}) = C(N_{\phi n}) \times 10^6, \quad C^0(M^0_{\phi n}) = C(M_{\phi n}) \times 10^6,$$
$$C^0(N^0_n) = C(N_n) \times 10^6, \quad C^0(Q^0_n) = C(Q_n) \times 10^6. \tag{25}$$

If, on the interval $s_1 \leqslant s \leqslant s_{N-1}$, we represent our accelerations in equations (8) by equations (14), we obtain explicit expressions for the variables $w_n(s, t)$, $u_{\phi n}(s, t)$, and $u_{\theta n}(s, t)$ on that spatial interval. We then have available 14 separate equations written for time t for each boundary to evaluate implicitly the remaining variables in our system of equations for the time t. To obtain our implicit equations for the boundaries s_0 and s_N, the accelerations will be represented typically by equation (15). The finite difference equations representing equations (8) and (9) together with the applicable computer program for both t_1 and t_2 are given in reference [25].

5. SELECTION OF MERIDIONAL AND TIME INCREMENTS

To solve our system of finite difference equations, choices must be made for the increments Δs, Δt, and the multipliers α_j of Δs which together with Δs define the meridional finite difference mesh as shown in Figure 4. These increments together with the multipliers α_j must have magnitudes which produce numerical stability of the finite difference solution. We expect the required relations between the time and spatial increments and the multipliers α_j to be dependent upon the formulation of the differential equations, the order of the finite difference representations used for the derivatives [13, 14], and the magnitudes and variations of α_j over the whole range of the finite difference mesh. For any given spatial mesh, we expect to find some value of $\Delta t(\mathrm{MAX})$ for which values of $\Delta t \leqslant \Delta t(\mathrm{MAX})$ will result in stable solutions and for which values of $\Delta t > \Delta t(\mathrm{MAX})$ will produce numerically unstable solutions.

The selection of the meridional increments $\alpha_j \Delta s$ will be based on the requirement that the finite difference solution for the static problem must converge to the true solution of the differential equations. Thus, since in this case we are solving a system of finite difference equations in only one independent variable, stability is divorced from our consideration of the choice of the increments $\alpha_j \Delta s$. We thus need only to choose the increments $\alpha_j \Delta s$ to minimize truncation and possibly round-off errors. We expect round-off errors to be significant as Δs approaches zero, and truncation errors will be significant if the $\alpha_j \Delta s$ are chosen to be too large. Upon the basis of static solutions obtained for typical shells, it appears that accurate static solutions are obtained if the increments $\alpha_j \Delta s$ are chosen to be one to four times the thickness of the shell. We will therefore generally choose the increments $\alpha_j \Delta s$ to lie within this range for the solution of our finite difference equations for the dynamic shell problem and then use in conjunction therewith a value of $\Delta t \leqslant \Delta t(\mathrm{MAX})$, where $\Delta t(\mathrm{MAX})$ will be found by an evaluation of the eigenvalues of the coefficient matrix for the displacements $w_n(s, t - \Delta t)$, $u_{\phi n}(s, t - \Delta t)$, and $u_{\theta n}(s, t - \Delta t)$ in our matrix equation for $w_n(s, t)$, $u_{\phi n}(s, t)$, and $u_{\theta n}(s, t)$ for trial values of Δt. We obtain our initial trial value of Δt for the coefficient matrix eigenvalue analysis by use of the empirical formula

$$\Delta t = (-0{\cdot}2809524 + 6{\cdot}7666667\bar{\Delta}s - 4{\cdot}5333333\bar{\Delta}s^2 + 3{\cdot}0476190\bar{\Delta}s^3)10^{-6}, \tag{26}$$

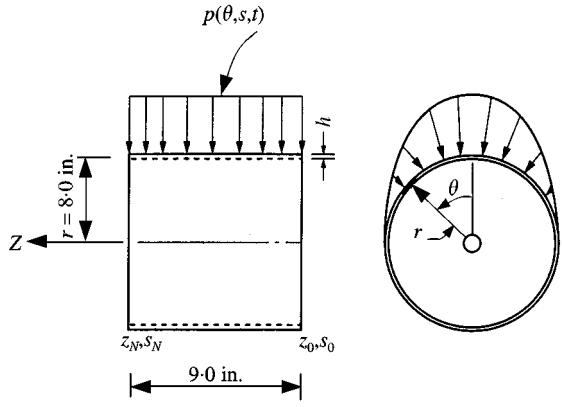

Figure 5. Example cylindrical shell with continuous loading. The loading $p(\theta, s, t) = -1000\cos\theta(-\pi/2 \leqslant \theta \leqslant \pi/2)$. The boundary conditions at s_0 are $w = 0$, $u_\phi = 0$, $u_\theta = 0$, and $M_\phi = 0$. Boundary conditions at s_N are $w = 0$, $N_\phi = 0$, $u_\theta = 0$, and $M_\phi = 0$. The thickness $h = 0{\cdot}25$ in.

based on studies [23] of the cylindrical shell of Figure 5 and the parabolic shell of Figure 6 (which have been verified for the formulation of reference [25]), where

$$\bar{\Delta}s = \alpha_j \Delta s(\text{Min}). \tag{27}$$

To develop our criterion for numerical stability, we represent symbolically our explicit relations for the variables w_n, $u_{\phi n}$, and $u_{\theta n}$ on the interval $s_1 \leqslant s \leqslant s_{N-1}$ as

$$U(s, t) = G(s, \Delta s, \Delta t)U(s, t - \Delta t) - HU(s, t - 2\Delta t) + Z(s, t - \Delta t), \tag{28}$$

where

$$U(s, t) = [w_n(s_i, t), u_{\phi n}(s_i, t), u_{\theta n}(s_i, t)]^{\mathrm{T}} \quad (i = 1, \ldots, N - 1), \tag{29}$$

for which the three elements at s_i are repeated successively at each i to generate a column matrix of order $3N - 3$,

$$G(s, \Delta s, \Delta t) = [g_{ij}(s, \Delta s, \Delta t)] \quad (i = 1, \ldots, 3N - 3; j = 1, \ldots, 3N - 3), \tag{30}$$

$$U(s, t - \Delta t) = [w_n(s_i, t - \Delta t), u_{\phi n}(s_i, t - \Delta t), u_{\theta n}(s_i, t - \Delta t)]^{\mathrm{T}} \quad (i = 1, \ldots, N - 1), \tag{31}$$

$$H = I_{3N-3} = \text{unit diagonal matrix of order } 3N - 3, \tag{32}$$

$$U(s, t - 2\Delta t) = [w_n(s_i, t - 2\Delta t), u_{\phi n}(s_i, t - 2\Delta t),$$

$$u_{\theta n}(s_i, t - 2\Delta t)]^{\mathrm{T}} \quad (i = 1, \ldots, N - 1), \tag{33}$$

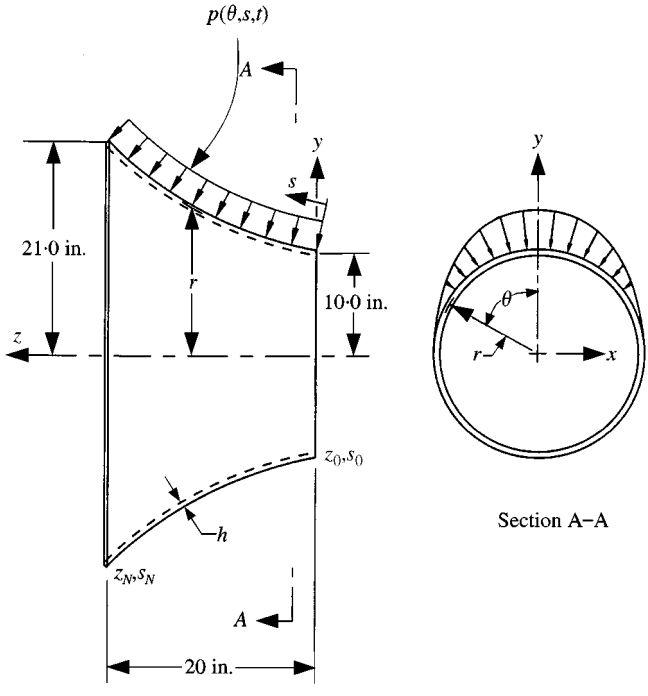

Figure 6. Example parabolic shell with continuous loading, $p(\theta, s, t) = -100\cos\theta(-\pi/2 \leqslant \theta \leqslant \pi/2)$; $r = 10 + 0{\cdot}15z + 0{\cdot}02z^2$. The boundary at s_0 is completely fixed, and the boundary at s_N is completely free. The thickness $h = 0{\cdot}10$ in.

$$Z(s, t - \Delta t) = [\text{displacement terms } (s_{-1}, t - \Delta t; s_0, t - \Delta t;$$

$$s_N, t - \Delta t; s_{N+1}, t - \Delta t)]^{\mathrm{T}}$$

$$+ [\text{loading and force terms } (s_i, t - \Delta t)]^{\mathrm{T}} \quad (i = 1, \ldots, N - 1). \quad (34)$$

We note that the $Z(s, t - \Delta t)$ column matrices of summed terms at each node point together with the terms for $U(s, t - 2\Delta t)$ will not enter into the analysis of the G matrix. Only the coefficients g_{ij} of the three fundamental variables w_n, $u_{\phi n}$, and $u_{\theta n}$ on the interval $s_1 \leqslant s \leqslant s_{N-1}$ constitute the elements of the G matrix. Thus, stability or instability of our calculations will be governed solely by the behavior of our solution as given by the matrix equation

$$U^*(s, t) = G(s, \Delta s, \Delta t)U(s, t - \Delta t) - HU(s, t - 2\Delta t). \quad (35)$$

The unit diagonal matrix H has eigenvalues $\beta_j = 1$ $(j = 1, 2, 3, \ldots, 3N - 3)$ and will not contribute to any numerical instability. Thus, as far as numerical stability or instability is concerned, we need only to evaluate the behavior of the matrix G.

The matrix G in equation (35) is a banded matrix the width of which depends upon the order of spatial finite difference representations used for the derivatives in our field equations. We may convert matrix G to diagonal form by the relation

$$GU(s, t - \Delta t) = \lambda IU(s, t - \Delta t), \tag{36}$$

where λ is any of $3N - 3$ eigenvalues of the matrix G, where I is the unit diagonal matrix of order $3N - 3$, and where $\lambda = \lambda(\Delta s, \Delta t)$.

Thus, we have

$$(G - \lambda I)U(s, t - \Delta t) = 0. \tag{37}$$

The eigenvalues λ_j and the eigenvectors V_j of the matrix G will be found from the condition that the determinant of the coefficient matrix for U vanishes. Thus,

$$|G - \lambda I| = 0. \tag{38}$$

The eigenvectors V_j are given by

$$V_j = C_j[W_{nj}(s_i, t - \Delta t), U_{\phi nj}(s_i, t - \Delta t), U_{\theta nj}(s_i, t - \Delta t)]^{\mathrm{T}}$$

$$(i = 1, \ldots, N - 1; j = 1, 2, 3, \ldots, 3N - 3), \tag{39}$$

where $W_{nj}(s_i, t - \Delta t)$, $U_{\phi nj}(s_i, t - \Delta t)$, and $U_{\theta nj}(s_i, t - \Delta t)$ represent the eigenvector displacements $w_n(s_i, t - \Delta t)$, $u_{\phi n}(s_i, t - \Delta t)$, and $u_{\theta n}(s_i, t - \Delta t)$ defining the shapes of the eigenvectors for the Fourier component n on the interval $s_1 \leqslant s \leqslant s_{N-1}$, and where the C_j are constants to be determined in each case to ensure that

$$\sum_{j=1}^{3N-3} V_j(s, t - \Delta t) = U(s, t - \Delta t). \tag{40}$$

Although they are not required for the purposes of this analysis, the $(3N - 3)$ C_j may be found by solution of the matrix equation

$$QC = U, \tag{41}$$

where

$$Q = [q_{kj}] \quad (k = 1, 2, 3, \ldots, 3N - 3; j = 1, 2, 3, \ldots, 3N - 3), \tag{42}$$

$$C = [C_1, C_2, C_3, \ldots, C_{3N-3}]^{\mathrm{T}}, \tag{43}$$

and where U is defined by equation (31).

The q_{kj} in equation (42) are the eigenvector shape values W_n, $U_{\phi n}$, and $U_{\theta n}$ given in equation (39).

We note in particular that each of the eigenvectors V_j constitutes individually a solution of the system of equations

$$GV_j = \lambda_j V_j \quad \text{(no summation on } j\text{)}. \tag{44}$$

From equation (38), we will obtain $3N-3$ eigenvalues λ_j and their associated eigenvectors V_j. In terms of λ_j and V_j, we have in lieu of equations (35) the following equation for $U^*(s, t)$:

$$U^*(s, t) = \sum_{j=1}^{3N-3} \lambda_j V_j(s, t - \Delta t) - HU(s, t - 2\Delta t), \tag{45}$$

where λ_j is the modulus of the real and imaginary, if any, eigenvalues λ_j (Re) and λ_j(Im) of the matrix G.

By comparing coefficients in equation (45) with the corresponding coefficients in equation (14) at times $(t - 2\Delta t)$, $(t - \Delta t)$, and t, it is clear that the solutions obtained by equation (28) will be stable if the maximum value of the eigenvalues of the matrix G is less than or equal to two, i.e.,

$$|\lambda(\max)| \leqslant 2. \tag{46}$$

We note that the elements g_{ij} of matrix G are functions of Δs and Δt. However, each of the elements g_{ii} along the diagonal of the matrix has an additive constant 2·0 for the displacement terms $w_n(s_j, t - \Delta t)$, $u_{\phi n}(s_j, t - \Delta t)$, and $u_{\theta n}(s_j, t - \Delta t)$, respectively, as given by our explicit equations for $w_n(s_j, t)$, $u_{\phi n}(s_j, t)$, and $u_{\theta n}(s_j, t)$. For any chosen spatial mesh, we will find some value of Δt for which $|\lambda(\text{MAX})|$ is equal to 2. Solutions will also be stable as we reduce Δt. As Δt is reduced, the elements g_{ij} off the diagonal are reduced in absolute value; and, similarly, the elements g_{ii} on the diagonal are altered in value. As Δt approaches zero, only the elements g_{ii} along the diagonal will be significant at a value of 2, and all eigenvalues of the matrix G will be equal to 2. As Δt is increased beyond the value Δt for which $|\lambda(\text{MAX})| = 2$, the elements g_{ij} of matrix G will increase in value and produce values for $|\lambda(\text{MAX})| > 2$, indicating unstable solutions.

The above development for a numerical stability criterion is applicable directly for either the symmetric or the antisymmetric Fourier components for $n \geqslant 1$. Separate developments for the symmetric and antisymmetric Fourier components for $n = 0$, resulting in the same criterion as above for numerical stability, may be found in reference [25].

To implement the above development, we have included in the computer program accompanying reference [25] the subroutine EIGNCX [27], which will determine all real and imaginary, if any, eigenvalues λ_j and the eigenvectors associated with the real matrix G. To illustrate results of stability studies for the cylindrical shell and loading shown in Figure 5, we assume that the initial displacements and velocities are zero. For the boundary conditions, we assume that w, u_ϕ, M_ϕ, and u_θ and zero at z_0 and that w, N_ϕ, M_ϕ, and u_θ are zero at z_N. We take for E a value of 30×10^6 lb/in^2 for γ a value of 0·2835 lb/in^3, and for ν a value of 0·30. We use only the symmetric Fourier components for $n = 0$ to 4. Thus, the four non-zero components entering into our evaluation are $p_0 = -318{\cdot}0$, $p_1 = -500{\cdot}0$, $p_2 = -212{\cdot}0$, and $p_4 = 42{\cdot}0$ lb/in^2. We show in Table 1 the results of our stability studies using the stability criterion of equation (46) for the nine different mesh spacings. The first four cases are for constant nodal point spacings, and the remaining cases involve variable spacings as sequenced in Figure 4 and shown in

TABLE 1

Stability limits for example cylindrical shell for $n = 0, 1, 2$ *and* 4

Mesh spacing case no.	N No. of spaces between s_0 and s_N	Δs (in)	Values of α_j	$\alpha_j \Delta s$(Min) (in)	Time increment Δt (10^{-6} s)	
					Stable	Unstable
1	144	0·0625	1·00, $1 \leqslant j \leqslant 148$	0·0625	$\leqslant$ 0·125	$\geqslant$ 0·150
2	72	0·125	1·00, $1 \leqslant j \leqslant 76$	0·125	$\leqslant$ 0·50	$\geqslant$ 0·52
3	36	0·25	1·00, $1 \leqslant j \leqslant 40$	0·25	$\leqslant$ 1·175	$\geqslant$ 1·200
4	18	0·50	1·00, $1 \leqslant j \leqslant 22$	0·50	$\leqslant$ 2·350	$\geqslant$ 2·375
5	52	0·25	0·50, $1 \leqslant j \leqslant 18$ 1·00, $19 \leqslant j \leqslant 38$ 0·50, $39 \leqslant j \leqslant 56$	0·125	$\leqslant$ 0·50	$\geqslant$ 0·52
6	44	0·25	0·50, $1 \leqslant j \leqslant 10$ 1·00, $11 \leqslant j \leqslant 38$ 0·50, $39 \leqslant j \leqslant 48$	0·125	$\leqslant$ 0·52	$\geqslant$ 0·54
7	44	0·25	0·25, $1 \leqslant j \leqslant 2$ 0·50, $3 \leqslant j \leqslant 10$ 1·00, $11 \leqslant j \leqslant 38$ 0·50, $39 \leqslant j \leqslant 46$ 0·25, $47 \leqslant j \leqslant 48$	0·0625	$\leqslant$ 0·50	$\geqslant$ 0·52
8	46	0·25	0·25, $1 \leqslant j \leqslant 4$ 0·50, $5 \leqslant j \leqslant 11$ 1·00, $12 \leqslant j \leqslant 39$ 0·50, $40 \leqslant j \leqslant 46$ 0·25, $47 \leqslant j \leqslant 50$	0·0625	$\leqslant$ 0·200	$\geqslant$ 0·225
9	52	0·25	0·25, $1 \leqslant j \leqslant 10$ 0·50, $11 \leqslant j \leqslant 14$ 1·00, $15 \leqslant j \leqslant 42$ 0·50, $43 \leqslant j \leqslant 46$ 0·25, $47 \leqslant j \leqslant 56$	0·0625	$\leqslant$ 0·125	$\geqslant$ 0·150

TABLE 2

Matrix G eigenvalues λ(MAX) *for case numbers* 3 *and* 8 *in Table* 1

Mesh spacing case no. (Table 1)	n	Time increment Δt (10^{-6} s)	λ(MAX)	Stability condition
3	0	1·175	1·99904	Stable
		1·200	2·13313	Unstable
3	1	1·175	1·99932	Stable
		1·200	2·13348	Unstable
3	2	1·175	1·99961	Stable
		1·200	2·13455	Unstable
3	4	1·175	1·99981	Stable
		1·200	2·13881	Unstable
8	0	0·200	1·99997	Stable
		0·225	2·89117	Unstable
8	1	0·200	1·99998	Stable
		0·225	2·89142	Unstable
8	2	0·200	1·99999	Stable
		0·225	2·89216	Unstable
8	4	0·200	1·99999	Stable
		0·225	2·89513	Unstable

Table 1. It is of interest to compare the results for Cases 7 and 8 in Table 1. For Case 7, $\alpha_j \Delta s$ (Min) occurs over only two spaces outside each boundary and stable solutions occur with $\Delta t \leqslant 0{\cdot}50 \times 10^{-6}$ s. For Case 8, $\alpha_j \Delta s$(Min) occurs over two spaces both outside and inside the boundaries. This resulted in a reduction of the stability limit to $\Delta t \leqslant 0{\cdot}200 \times 10^{-6}$ s. The validity of the results in Table 1 has been confirmed by actual running of the solutions. We show in Table 2 the maximum eigenvalues of matrix G for Cases 3 and 8 of Table 1 for each of the Fourier components $n = 0$, 1, 2, and 4.

To investigate the stability conditions for the parabolic shell and loading shown in Figure 6, we take the initial displacements and velocities to be zero. We assume for the boundary conditions that w, u_ϕ, u_θ, and β_ϕ are zero at z_0 and that Q, N_ϕ, N, and M_ϕ are zero at z_N. We assume a value of 30×10^6 lb/in^2 for E, a value of 0·2835 lb/in^3 for γ, and a value of 0·30 for ν. For the given conditions, only the equations containing the symmetric Fourier components enter into our evaluation. We consider only the Fourier components for $n = 0$ to 8 and have for the non-zero components the values $p_0 = -31{\cdot}8$, $p_1 = -50{\cdot}0$, $p_2 = -21{\cdot}2$, $p_4 = 4{\cdot}2$, $p_6 = -1{\cdot}8$, and $p_8 = 1{\cdot}0$ lb/in^2 for the loading. We show in Table 3 the results of our stability studies using the stability criterion of equation (46) for four different mesh spacings. The first three cases are for constant nodal point spacings, and the fourth case involves variable nodal point spacings as sequenced in Figure 4 and shown in

TABLE 3

Stability limits for example parabolic shell for $n = 0, 1, 2, 4, 6$ *and* 8

Mesh spacing case no.	N No. of space between s_0 and s_N	Δs (in)	Values of α_j	$\alpha_j \Delta s$(Min) (in)	Time increment Δt (10^{-6} s)	
					Stable	Unstable
1	144	0·16100671	$1{\cdot}00,\ 1 \leqslant j \leqslant 148$	0·16100671	$\leqslant 0{\cdot}75$	$\geqslant 0{\cdot}76$
2	72	0·32201342	$1{\cdot}00,\ 1 \leqslant j \leqslant 76$	0·32201342	$\leqslant 1{\cdot}50$	$\geqslant 1{\cdot}52$
3	36	0·64402685	$1{\cdot}00,\ 1 \leqslant j \leqslant 40$	0·64402685	$\leqslant 3{\cdot}00$	$\geqslant 3{\cdot}02$
4	90	0·25761073	$1{\cdot}25,\ 1 \leqslant j \leqslant 56$ $0{\cdot}625,\ 57 \leqslant j \leqslant 94$	0·16100671	$\leqslant 0{\cdot}76$	$\geqslant 0{\cdot}78$

Table 3. Again, the validity of these results has been confirmed by actually running the solutions. We show in Table 4 the maximum eigenvalues of matrix G for Cases 3 and 4 of Table 3 for each of the Fourier components $n = 0, 1, 2, 4, 6$, and 8. It can be seen from Tables 2 and 4 that the eigenvalues λ(MAX) increase gradually as the Fourier number n increases from 0 to the maximum value of n. Thus, we expect stability (or instability) to be governed by the maximum value of n which is used in our finite difference analysis. It is not, therefore, expected to be necessary to determine the eigenvalues for any of the Fourier components other than the maximum value of n used in our shell analysis.

6. RESULTS FOR A PARABOLIC SHELL

The purpose of the present report was the development of finite difference procedures for either the static or dynamic analysis of general rotationally symmetric shells which would provide a more efficient solution for shell variables at and near the boundaries of the shell than obtainable by use of a constant finite difference nodal point spacing used in other formulations. To obtain this more efficient solution, we envision and have incorporated in the governing finite difference equations the capability to specify a variable node point spacing over the entire finite difference mesh covering the interval $s_{-2} \leqslant s \leqslant s_{N+2}$. We expect its advantages to be realized most effectively by specifying a finer mesh segment at and near the shell boundaries and a coarser mesh segment away from the boundaries. To show the effects of the variable spacing at and adjacent to the boundaries, we show examples of both static and dynamic solutions found by using both a constant and a variable nodal point spacing when applied to the parabolic shell and loading shown in Figure 6. It will be seen that essentially the same solutions may be obtained with somewhat less nodal points on the shell meridian by use of a variable and smaller spacing near the boundaries in lieu of a constant spacing of the finite difference nodal points over the full length of the shell meridian.

As an illustration of static solutions, we analyze the parabolic shell for the loading shown in Figure 6 when the loading is statically applied. In all cases, we

TABLE 4

Matrix G eigenvalues λ(MAX) *for case numbers* 3 *and* 4 *in Table* 3

Mesh spacing case no. (Table 2)	n	Time increment Δt (10^{-6} seconds)	λ(MAX)	Stability condition
3	0	3·00	1·99936	Stable
		3·02	1·99936	Stable
3	1	3·00	1·99942	Stable
		3·02	1·99941	Stable
3	2	3·00	1·99960	Stable
		3·02	1·99960	Stable
3	4	3·00	1·99981	Stable
		3·02	1·99981	Stable
3	6	3·00	1·99987	Stable
		3·02	1·99987	Stable
3	8	3·00	1·99988	Stable
		3·02	2·00188	Unstable
4	0	0·76	1·99996	Stable
		0·78	2·21012	Unstable
4	1	0·76	1·99996	Stable
		0·78	2·21015	Unstable
4	2	0·76	1·99997	Stable
		0·78	2·21023	Unstable
4	4	0·76	1·99999	Stable
		0·78	2·21054	Unstable
4	6	0·76	1·99999	Stable
		0·78	2·21107	Unstable
4	8	0·76	1·99999	Stable
		0·78	2·21181	Unstable

assume that w, u_ϕ, u_θ, and β_ϕ are zero at z_0 and that Q, N_ϕ, N, and M_ϕ are zero at z_N. We take for E a value of 30×10^6 lb/in^2, for γ a value of 0·2835 lb/in^3 and for v a value of 0·30. We use only the Fourier components for $n = 0$ to 8. Thus, the six non-zero components entering into the solution are $p_0 = -31{\cdot}8$, $p_1 = -50{\cdot}0$, $p_2 = -21{\cdot}2$, $p_4 = 4{\cdot}2$, $p_6 = -1{\cdot}8$, and $p_8 = 1{\cdot}0$ lb/in^2. We make our analyses for four different mesh spacing layouts described as Cases 1–4 in Table 3. The first three cases are for constant node point spacings of 0·1610, 0·3220, and 0·6440 in., respectively. Case 4 constitutes the variable node point spacing layout. We show in Table 5, for each of the four mesh spacing layouts, values of $w(s)$. It can be seen by inspection of the results in Table 5 that results in reasonably good agreement with each other may be found with any of the four mesh spacing layouts. It is seen also

TABLE 5

Example parabolic shell static solutions for $w(s)$ at $\theta = 0$ for $n = 0, 1, 2, 4, 6$ and 8 for constant and variable nodal point spacings

	$w(s)$ (in)			
	constant spacings			
s (in)	$\Delta s = 0{\cdot}1610$ in	$\Delta s = 0{\cdot}3220$ in	$\Delta s = 0{\cdot}6440$ in	Variable spacing (Table 3, Case 4)
0·000	$-1{\cdot}9116 \times 10^{-17}$	$-2{\cdot}5294 \times 10^{-19}$	0.	$-4{\cdot}6992 \times 10^{-18}$
2·576	$-1{\cdot}3164 \times 10^{-2}$	$-1{\cdot}3131 \times 10^{-2}$	$-1{\cdot}3012 \times 10^{-2}$	$-1{\cdot}3137 \times 10^{-2}$
5·152	$-2{\cdot}6051 \times 10^{-2}$	$-2{\cdot}6029 \times 10^{-2}$	$-2{\cdot}5945 \times 10^{-2}$	$-2{\cdot}6034 \times 10^{-2}$
7·728	$-3{\cdot}9054 \times 10^{-2}$	$-3{\cdot}9054 \times 10^{-2}$	$-3{\cdot}9050 \times 10^{-2}$	$-3{\cdot}9051 \times 10^{-2}$
10·304	$-5{\cdot}2138 \times 10^{-2}$	$-5{\cdot}2150 \times 10^{-2}$	$-5{\cdot}2193 \times 10^{-2}$	$-5{\cdot}2142 \times 10^{-2}$
12·880	$-6{\cdot}5188 \times 10^{-2}$	$-6{\cdot}5197 \times 10^{-2}$	$-6{\cdot}5229 \times 10^{-2}$	$-6{\cdot}5190 \times 10^{-2}$
15·456	$-7{\cdot}7863 \times 10^{-2}$	$-7{\cdot}7863 \times 10^{-2}$	$-7{\cdot}7866 \times 10^{-2}$	$-7{\cdot}7861 \times 10^{-2}$
18·032	$-9{\cdot}0059 \times 10^{-2}$	$-9{\cdot}0054 \times 10^{-2}$	$-9{\cdot}0048 \times 10^{-2}$	$-9{\cdot}0056 \times 10^{-2}$
20·608	$-1{\cdot}0202 \times 10^{-1}$	$-1{\cdot}0202 \times 10^{-1}$	$-1{\cdot}0204 \times 10^{-1}$	$-1{\cdot}0202 \times 10^{-1}$
23·184	$-1{\cdot}1394 \times 10^{-1}$	$-1{\cdot}1395 \times 10^{-1}$	$-1{\cdot}1401 \times 10^{-1}$	$-1{\cdot}1395 \times 10^{-1}$

TABLE 6

Example parabolic shell dynamic solutions for $w(s_N, t)$ at $\theta = 0$ for $n = 0, 1, 2, 4, 6$ and 8 for constant and variable nodal point spacings

	$w(s_N, t)$ (in)			
	Constant spacings			
t (10^{-5} s)	$\Delta s = 0{\cdot}1610$ in $\Delta t = 0{\cdot}75 \times 10^{-6}$ s	$\Delta s = 0{\cdot}3220$ in $\Delta t = 1{\cdot}50 \times 10^{-6}$ s	$\Delta s = 0{\cdot}6440$ in $\Delta t = 3{\cdot}00 \times 10^{-6}$ s	Variable spacing (Table 3, Case 4) $\Delta t = 0{\cdot}75 \times 10^{-6}$ s
0	0	0	0	0
12·0	$-9{\cdot}2422 \times 10^{-3}$	$-9{\cdot}2343 \times 10^{-3}$	$-9{\cdot}2070 \times 10^{-3}$	$-9{\cdot}2423 \times 10^{-3}$
24·0	$-3{\cdot}2779 \times 10^{-2}$	$-3{\cdot}2757 \times 10^{-2}$	$-3{\cdot}2674 \times 10^{-2}$	$-3{\cdot}2779 \times 10^{-2}$
36·0	$-6{\cdot}5527 \times 10^{-2}$	$-6{\cdot}5502 \times 10^{-2}$	$-6{\cdot}5395 \times 10^{-2}$	$-6{\cdot}5531 \times 10^{-2}$
48·0	$-1{\cdot}0262 \times 10^{-1}$	$-1{\cdot}0260 \times 10^{-1}$	$-1{\cdot}0247 \times 10^{-1}$	$-1{\cdot}0264 \times 10^{-1}$
60·0	$-1{\cdot}3686 \times 10^{-1}$	$-1{\cdot}3677 \times 10^{-1}$	$-1{\cdot}3663 \times 10^{-1}$	$-1{\cdot}3674 \times 10^{-1}$
72·0	$-1{\cdot}6378 \times 10^{-1}$	$-1{\cdot}6376 \times 10^{-1}$	$-1{\cdot}6369 \times 10^{-1}$	$-1{\cdot}6384 \times 10^{-1}$
84·0	$-1{\cdot}8679 \times 10^{-1}$	$-1{\cdot}8663 \times 10^{-1}$	$-1{\cdot}8659 \times 10^{-1}$	$-1{\cdot}8670 \times 10^{-1}$
96·0	$-2{\cdot}0529 \times 10^{-1}$	$-2{\cdot}0505 \times 10^{-1}$	$-2{\cdot}0526 \times 10^{-1}$	$-2{\cdot}0506 \times 10^{-1}$
108·0	$-2{\cdot}1767 \times 10^{-1}$	$-2{\cdot}1793 \times 10^{-1}$	$-2{\cdot}1748 \times 10^{-1}$	$-2{\cdot}1788 \times 10^{-1}$
120·0	$-2{\cdot}2253 \times 10^{-1}$	$-2{\cdot}2204 \times 10^{-1}$	$-2{\cdot}2160 \times 10^{-1}$	$-2{\cdot}2223 \times 10^{-1}$

that more accurate results on and near the boundaries may be achieved by use of smaller spacings there in conjunction with wider spacings away from the boundaries with appreciably less node points in the mesh than required by a smaller constant spacing mesh.

As an illustration of the effects of a variable nodal point spacing on dynamic solutions, we analyze the parabolic shell of Figure 6 for the dynamic loading and boundary conditions shown in Figure 6. In all cases, all other conditions are the same as given above for the static loading illustration. We show in Table 6, for each of the four mesh spacing layouts, values of $w(s_N, t)$. It can be seen by inspection of the results given in Table 6 that displacements on the boundaries may be obtained more accurately by use of smaller spacings at and near the boundaries in conjunction with larger spacings elsewhere with markedly less node points in the mesh than needed by a smaller constant spacing mesh.

7. CONCLUSIONS

The purpose of this article was to present the development of finite difference procedures for either the static or the dynamic analysis of rotationally symmetric shells which provide a more efficient solution for the shell variables at and near the boundaries than obtainable by use of a constant nodal point spacing between the boundaries as used in other formulations. This has been achieved by formulating the system of finite difference equations to permit an arbitrary nodal point spacing in the finite difference mesh over the entire spatial interval $s_{-2} \leqslant s \leqslant s_{N+2}$. It is clear that a constant nodal point spacing may also be specified in any particular case if desired. In practice, the solution efficiency will be obtained by specifying a nodal point spacing with a finer mesh segment near the boundaries and a coarser mesh segment away from the boundaries of the shell.

We have shown in Tables 5 and 6, respectively, comparison static and dynamic solutions (based upon constant versus variable nodal point spacings) for the parabolic shell, loading, and boundary conditions described in Figure 6. It is seen by a study of these results that essentially the same solutions may be obtained with considerably less nodal points on the shell meridian by use of a variable and smaller spacing near the boundaries in conjunction with a coarser mesh away from the boundaries in lieu of a constant nodal point spacing over the full length of the shell meridian.

The utility of the accompanying computer program has also been enhanced by including therein an explicit empirical relation for a trial time increment Δt in terms of the minimum spatial increment $\alpha_j \Delta_s$ (Min). This empirical relation has been based upon numerical stability studies for both the cylindrical shell shown in Figure 5 and the parabolic shell described in Figure 6 as reported in section 5. The major enhancement of this investigation is, however, the development and implementation into the analytical program, which accompanies the report, of a stability criterion which will determine numerical stability or instability for given choices of Δt and spatial meshes prior to performing any extensive calculations. The validity of the developed criterion has been confirmed by comparison of the results of applying the stability criterion with results of actual solutions for both the cylindrical shell and the parabolic shell examples used herein.

It is of interest to compare the values in Tables 5 and 6 with the corresponding values found in reference [23]. Values for a constant node point spacing are, as expected, identical for the two formulations. In the cases for a variable node point

spacing, the values in Tables 5 and 6 agree to 4 significant digits with the results found in reference [23].

We conclude that the finite difference procedures developed here provide optimal efficiency for the finite difference analysis of rotationally symmetric shells using variable node point spacings under either static or dynamic loadings.

ACKNOWLEDGMENTS

Grateful acknowledgement is extended to Mr. Michael D. Parker, U.S. Army Aviation and Missile Command, who implemented the author's computer program of reference [25], obtained all solutions given therein and included herein, and engaged in valuable discussions with the author during the program development.

Recognition is also given to the contribution of Mr. William R. Sellers, Jr. (deceased), formerly an employee of the US Army Missile Command, who in 1988 developed the program subroutine EIGNCX for the numerical evaluation of the real and imaginary components of the eigenvalues and eigenvectors of a general matrix.

REFERENCES

1. R. K. Penny 1961 *Journal of Mechanical Engineering Science* **3**, 369–377. Symmetric bending of the general shell of revolution by finite difference methods.
2. P. P. Radkowski, R. M. Davis, and M. R. Bolduc 1962 *ARS Journal* **32**, 36–41. Numerical analysis of equations of thin shells of revolution.
3. B. Budiansky and P. P. Radkowski 1963 *AIAA Journal* **1**, 1833–1842. Numerical analysis of unsymmetrical bending of shells of revolution.
4. A. Kalnins 1964 *Transactions ASME* 31*E Journal of Applied Mechanics* **3**, 467–476. Analysis of shells of revolution subjected to symmetrical and nonsymmetrical loads.
5. J. H. Percy, T. H. H. Pian, S. Klein, and D. R. Navaratna 1965 *AIAA Journal* **3**, 2138–2145. Application of matrix displacement method to linear elastic analysis of shells of revolution.
6. A. Kalnins 1964 *Journal of Acoustic Society of America* **36**, 1355–1365. Free vibration of rotationally symmetric shells.
7. H. Kraus and A. Kalnins 1965 *Journal of Acoustical Society of America* **38**, 994–1002. Transient vibration of thin elastic shells.
8. S. Klein 1966 *Shock and Vibration Bulletin* **35**, 27–44. Vibrations of multi-layer shells of revolution under dynamic and impulsive loadings.
9. T. A. Smith 1970 *U.S. Army Missile Command Technical Report RS-TR*-70-5, *Redstone Arsenal, Alabama.* Numerical solution for the dynamic response of rotationally symmetric shells of revolution under transient loadings.
10. T. A. Smith 1971 *AIAA Journal* **9**, 637–643. Numerical analysis of rotationality symmetric shells under transient loadings.
11. T. A. Smith 1973 *U.S. Army Missile Command Technical Report RL*-73-9, *Redstone Arsenal, Alabama.* Implicit high order finite difference analysis of rotationally symmetric shells.
12. H. Radwan and J. Genin 1975 *International Journal of Non-linear Mechanics* **10,** 15–29. Nonlinear modal equations for thin elastic shells.
13. T. A. Smith 1977 *U.S. Army Missile Research and Development Command Technical Report TL*-77-1, *Redstone Arsenal, Alabama.* Explicit high order finite difference analysis of rotationally symmetric shells.

14. T. A. Smith 1980 *AIAA Journal* **18**, 309–317. Explicit high-order finite-difference analysis of rotationally symmetric shells.
15. Y. B. Chang, T. Y. Yang, and W. Soedel 1983 *Journal of Sound and Vibration* **86**, 523–538. Linear dynamic analysis of revolutional shells using finite elements and modal expansion.
16. T. A. Smith 1983 *U.S. Army Missile Command Technical Report RL*-83-5, *Redstone Arsenal Alabama.* Finite difference analysis of rotationally symmetric shells under discontinuous distributed loadings.
17. T. A. Smith 1987 *AIAA Journal* **25**, 1611–1621. Finite difference analysis of rotationally symmetric shells under discontinuous distributed loadings.
18. T. A. Manteuffel and A. B. White Jr. 1986 *Mathematics of Computation* **47**, 511–535. The numerical solution of second-order boundary value problems on nonuniform meshes.
19. T. A. Smith 1991 *U.S. Army Missile Command Technical Report RD-ST*-91-1, *Redstone Arsenal, Alabama.* Dynamic Analysis of rotationally symmetric shells by the modal superposition method.
20. C. H. Norris, R. J. Hansen, M. J. Holley, Jr., J. M. Biggs, S. Namyet, and J. K. Minami 1959 *Structural Design for Dynamic Loads.* New York: McGraw-Hill Book Company, Inc.
21. T. A. Manteuffel and A. B. White Jr. 1992 *SIAM Journal of Numerical Analysis* **29**, 1321–1346. A calculus of difference schemes for the solution of boundary-value problems on irregular meshes.
22. T. A. Smith 1994 *U.S. Army Missile Command Technical Report RD-ST*-94-12, *Redstone Arsenal, Alabama.* Improved explicit high-order finite difference analysis of rotationally symmetric shells.
23. T. A. Smith 1995 *U.S. Army Missile Command Technical Report RD-ST*-95-15, *Redstone Arsenal, Alabama.* Finite difference analysis of rotationally symmetric shells using variable node point spacings.
24. T. A. Smith 1997 *U.S. Army Aviation and Missile Command Technical Report RD-ST*-97-5, *Redstone Arsenal, Alabama.* Improved numerical analysis of rotationally symmetric shells using eight first-order field equations.
25. T. A. Smith 1998 *U.S. Army Aviation and Missile Command Technical Report RD-PS*-99-1, *Redstone Arsenal, Alabama.* Finite difference analysis of rotationally symmetric shells using variable node point spacings and incorporating matrix stability analysis.
26. E. Reissner 1941 *American Journal of Mathematics* **63**, 177–184. A new derivation of the equations for the deformation of elastic shells.
27. W. R. Sellers Jr 1988 *U.S. Army Missile Command Letter Report AMSMI-RD-SS*-88-25, *Redstone Arsenal, Alabama.* A mathematical library for your PC.

APPENDIX A: NOMENCLATURE

$A_1, \ldots, A_{10}$	parameters defining the coefficients of the variables in equation (8a)
$B_1, \ldots, B_{13}$	parameters defining the coefficients of the variables in equation (8b)
C	coefficients of the force variables $N_{\phi n}$, $M_{\phi n}$, N_n, and Q_n in the finite difference equations obtained before change of force variables
C^0	coefficients of the modified force variables $N^0_{\phi n}$, $M^0_{\phi n}$, N^0_n, and Q^0_n in the governing finite difference equations
$C_1, \ldots, C_9$	parameters defining the coefficients of the variables in equation (8c)
D	flexural rigidity of the shell, $Eh^3/12(1-\nu^2)$
$D_1, \ldots, D_{50}$	parameters defining the coefficients of the variables in equations (9) and (10)
E	Young's modulus
g	acceleration constant
h	thickness of the shell

K	extensional rigidity of the shell, $Eh/(1-\nu^2)$
m_θ, m_ϕ	moments of the mechanical surface loads
$M_\theta, M_\phi, M_{\theta\phi}$	moment stress resultants
$M^0_{\phi n}$	$M_{\phi n} \times 10^{-6}$
n	integer, designating the nth Fourier component
N, Q	effective shear resultants
N^0_n, Q^0_n	$N_n \times 10^{-6}$ and $Q_n \times 10^{-6}$
$N_\theta, N_\phi, N_{\theta\phi}$	membrane stress resultants
$N^0_{\phi n}$	$N_{\phi n} \times 10^{-6}$
p, p_θ, p_ϕ	components of the mechanical surface loads
Q_θ, Q_ϕ	transverse stress resultants
r	distance of point on the middle surface of the shell from the axis of symmetry
R_θ, R_ϕ	principal radii of curvature of the middle surface of the shell
s	distance from an arbitrary origin along the meridian of the shell in the positive direction of ϕ
Δs	reference spacing between node points in the meridional finite difference mesh
t	independent time variable
Δt	increment of the time variable t
T_0, T_1	integrated values of temperature resultants
u_θ, u_ϕ, w	components of displacement of the middle surface of the shell
z	distance of point on the middle surface of the shell measured from the origin along the axis of symmetry
α_j	multipliers of reference spacing Δs for obtaining variable node point spacings in the finite difference mesh
β_θ, β_ϕ	angles of rotation of the normal to the middle surface of the shell
γ	weight of shell material per unit volume
θ, ϕ, ρ	coordinates of any point of the shell
ν	Poisson's ratio